



# Influence of turbine blade geometry on thickness of TBCs deposited by VPA and PS-PVD methods

**M. Góral\*, J. Sieniawski, S. Kotowski, M. Pytel, M. Masłyk**

Department of Materials Science, Rzeszow University of Technology,  
Al. Powstańców Warszawy 12, 35-959 Rzeszów, Poland

\* Corresponding e-mail address: mgoral@prz.edu.pl

Received 05.01.2012; published in revised form 01.03.2012

## ABSTRACT

**Purpose:** The authors presented in the article the influence of the jet engine turbine blade profile on the thickness and microstructure of thermal barrier coatings.

**Design/methodology/approach:** The assessment of model blade made of ZS6K alloy used in the first stage of the turbine engine was performed. The diffusion aluminide coating as well as the thermal barrier coating were deposited on the blade surface with a use of the out of pack method. The zirconia stabilized by yttrium oxide coating was deposited by PS-PVD method. The research was performed with a use of light- and scanning microscopy.

**Findings:** It has been proven, that the thickest coating was found on the leading edge and trailing edge of the blade. In those places the coating thickness was approx. 20-30% larger than in the other areas on turbine blade.

**Research limitations/implications:** The research was performed with a use of light- and scanning microscopy.

**Practical implications:** The obtained results indicate that it is possible to create the thermal barrier coating by PS-PVD process on the first stage turbine blades of the aircraft engine. It indicates the possibility of application of this process in the industrial practice.

**Originality/value:** The new method for TBC coating production were used.

**Keywords:** Metallic alloys; Ceramics and glasses; Corrosion; Erosion

**Reference to this paper should be given in the following way:**

M. Góral, J. Sieniawski, S. Kotowski, M. Pytel, M. Masłyk, Influence of turbine blade geometry on thickness of TBCs deposited by VPA and PS-PVD methods, Archives of Materials Science and Engineering 54/1 (2012) 22-28.

## MATERIALS

### 1. Introduction

Resistance of thermal barrier in nickel alloys applied in hot section elements of the aircraft engine to dangerous oxidation and hot corrosion largely depends on their chemical composition. Many alloy additions which improve thermal barrier affect

mechanical properties of alloys. The higher level of chromium results in alloy's increased vulnerability to corrosion, while it becomes more brittle and has less load carrying capacity.

While additions such as tungsten, vanadium and molybdenum improve alloy's mechanical properties, the increased content of these elements results in lower resistance to hot corrosion.

An ideal solution may be the use of thermal barrier coatings. There are three major types of protective coatings: diffusion, aluminide, and TBCs. On surfaces of Al- or Cr-enriched alloys  $\text{Cr}_2\text{O}_3$  or  $\text{Al}_2\text{O}_3$  oxide coatings are formed.

As long as concentration of these elements in alloys' chemical composition exceeds a certain level (approx. 6%), a protective oxide coating (TGO- thermally grown oxide) is formed on the surface.

The chromium oxide coating can grow quite quickly, however, at the temperature above  $1000^\circ\text{C}$  it triggers forming a compound  $\text{CrO}_3$  [1,2].

In order to improve coating's properties, additions of chemical elements are used so as to modify layers. Platinum addition to diffusive coatings boosts aluminium diffusion to the alloy's inner part as well as improves its resistance to oxidation. Forming of aluminide diffusion coatings can be achieved with the use of two methods: a low activity process (performed at high temperatures -  $1050\text{-}1100^\circ\text{C}$ ) or high activity process (performed at lower temperatures -  $700\text{-}950^\circ\text{C}$ ). Both processes differ in deposition parameters and its results - a different microstructure of the deposited coating and its properties. In a high activity process (performed at a low temperature), the protective coating grows beyond the original alloy surface, and in-core aluminium diffusion takes place. The coating is made up from  $\text{Ni}_2\text{Al}_3$  and  $\text{NiAl}$  phases. A diffusion annealing process usually follows aluminisation, in order to achieve a homogenous  $\text{NiAl}$  phase. During this process some noticeable carbides and other precipitates are formed close to the original surface base. This effect is harmful as it affects material resistance to corrosion and oxidation. In a low activity process the aluminium coating grows above the original basis surface. The coating is formed through from-the-core diffusion. The coating structure is made up from the  $\text{NiAl}$  phase mainly. In the low activity process a thicker diffusion area in the coating can be observed. Due to the coating formation through the outward nickel diffusion, a lower level of inclusions in the coating section is observed. Both types of coatings produced in these processes can be platinum modified. The  $(\text{Ni,Pt})\text{Al}$  phases and double  $(\text{Ni,Pt})\text{Al} + \text{PtAl}_2$  phase are formed. Too high a level of Pt in the coating increases its brittleness [3-5].

Multicomponent MCrAlY ( $M = \text{Fe, Co, Ni}$ ) coatings are the adhesive coating type. The coating composition comprises metal ( $\text{Ni,Co,Fe}$ ), chromium, aluminium and a small amount of yttrium. Heat-resistant MCrAlY coatings were developed by Pratt & Whitney. The FeCrAlY coating, developed in the late 1960's, was the first coating which received a patent and was used for commercial purposes. Subsequently, other types of cobalt and nickel-based coatings as well as the NiCoCrAlY coatings were developed [6].

Compared to diffusion coatings, these MCrAlYs are independent of the base alloy. Chemical composition of the coating as well as individual content of each element can be specifically determined depending on the degradation mechanism to which it is going to be exposed. The coating composition comprises 4 or 5 elements mostly. Chromium (17-25%) makes the coating resistant to corrosion and oxidation.

Aluminium (8-12%) forms a protective oxide layer, while less than 1% of Y, Hf, Zr protects the coating from peeling off and ensures its ductility. After deposition and thermal treatment, the coating has the two-phase  $\beta + \gamma$  ( $\text{NiAl} + \text{Ni}$ ) microstructure.

The  $\beta$  phase is an aluminium source for the oxide layer, while the  $\gamma$  phase ensures its ductility and resistance to thermal fatigue. Effectiveness of the MCrAlY coating results from its compatibility with the base and also from the fact that the layer does not affect properties of the alloy on which it has been deposited [2,6].

MCrAlY- type coatings are used in thermal barrier coating of components. Thermal barrier always comprises 2 layers: an external ceramic layer and an internal MCrAlY layer which provides anti-corrosion protection and ensures appropriate adhesion of the ceramic coating to the base. In order to achieve such a result, it is important to form the right microstructure and quality of the base.

Depending on requirements, appropriate technologies are used for deposition of such coatings. The EB-PVD method (Electron Beam Physical Vapour Deposition) used to be popular at first but due to its costly application alternative technologies of deposition, that is the APS (Air plasma spraying) method and the HVOF (high-velocity oxy-fuel) method were developed. Application of Thermal Barrier Coating's system (TBC's) decrease the base material temperature. This in turn allows for increasing the engine working temperature and turbine performance, improving its efficiency and reducing emission of harmful  $\text{NO}_x$  oxides. Application of thermal barrier in connection with internal and external cooling system using cold air from cooling channels helps to lower to blade base by approx.  $165^\circ\text{C}$  [2].

A typical TBC's coating consists of 2 major layers. The first layer is typical MCrAlY coating used to protect the material from hot corrosion. The external layer of thermal barrier is ceramic coating made of zirconium oxide stabilized by 7-8% yttrium oxide. Ceramic coating is deposited with the use of the physical vaporation method (EB-PVD). Depending on a deposition method, there can be obtained coatings of various microstructure and of various properties. In case of thermal barrier, thermal conductivity is an important parameter. It has been proven that microstructure can largely influence the thermal conductivity factor in coating [2,7].

In the EB-PVD method, vaporization takes place at a high temperature (approx.  $1000^\circ\text{C}$ ). Cleaned and prepared for coating, components are placed in a special vacuum chamber, where they are heated to the temperature of approx.  $1000^\circ\text{C}$ . During this process a layer of protective oxides (TGO) is formed. Next, the components are placed in another chamber where an electron beam is used to vaporize zirconium oxide (7YSZ), which then settles on the component. Average velocity of coating settling is 2-6  $\mu\text{m}$  per minute. Some sensitive components of an engine may require additional thermal treatment and finishing work. Coating microstructure formed in such a process has a column structure. Individual grains are arranged perpendicularly to the material surface, in accordance with the temperature gradient, what results in less efficiency of the coating since it has a higher thermal conductivity coefficient (1.71 W/mK) than plasma sprayed coatings. Improved mechanical properties are an advantage of this microstructure [2,8].

The use of the air plasma spraying method (APS) [9] has many characteristics common with the HVOF method. In the APS method, feed stock outside the plasma burner reach are placed in a protective gas atmosphere (e.g. Ar) or in vacuum. This limits the amount of oxygen in coating, which can affect protective properties of the coating. The coating microstructure formed with the use of

this method is noticeably porous, with pore size of up to 20 $\mu$ m. Pore edges are arranged parallel to the base, what results in a low thermal conductivity factor (0.9-1.1 W/mK) of the coating. This type of TBC was characterized by lower thermal conductivity in comparison with EB-PVD-made ceramic coatings. [2,9].

In the HVOF method a mixture of oxygen and fuel is fed into a spray pistol (hydrogen, methane, propane, propylene or kerosene depending on the pistol type), where it is combusted in a combustion chamber and then supplemented with a MCrAlY- alloy powder. The resultant combustion products travel through a special nozzle at a 1000-1500 m/s speed and the temperature of 2800°C. At the jet velocity, the powder feed stock is sprayed onto the surface and forms heat-resistant MCrAlY coating. [10-13].

## 2. Experimental

Research into aluminide coatings and TBC coating was carried out on a second stage turbin blade made of ZS6K alloy, which composition has been shown in Table 1.

Table 1.  
Chemical composition of the ZS6K alloy

Element,	C	Cr	Al	Ti	Mo	W	Co	Fe	Ni
wt.%	0.14	10.2	5.3	2.8	3.7	5.2	4.7	1.5	Bal.

A gas phase aluminising method was used to cover the blades with diffusion aluminide coating. The 4-hour-long procedure was run at the temperature of 1000°C in argon atmosphere. Ceramic coating was deposited on a sandpapered aluminide coating.

The LPPS Thin Film equipment manufactured by Sulzer-Metco was used during the Plasma Spray Physical Vapour Deposition method.

Research methodology was the same for each blade. A blade airfoil was cut at  $\frac{3}{4}$  of its height (counting from the lock). Thickness measurements were taken in the section in spots indicated as KS, KN, KS-G, KS-D as well as G and D in Fig. 1.

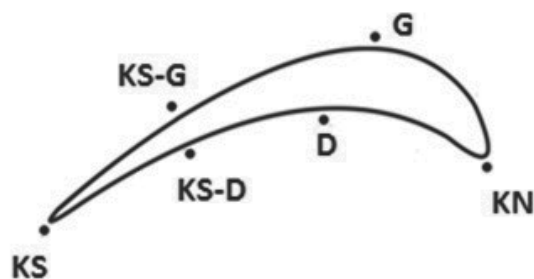


Fig. 1. Thickness measurement spots for aluminide layer and ceramic layer in the blade section. Description: to Fig. 1: KN - leading edge; G - blade top, the profile's maximum thickness point; KS-G - blade top, approx. 1/3 of the length from the trailing edge; KS - trailing edge; KS-D - blade platform, approx. 1/3 of the length from the trailing edge; D - blade platform, the profile's maximum thickness point

Metallographic specimens for microstructure analysis were prepared in the following manner: electroless nickel-plating of blades, cutting of the blades, inclusion of samples, sandpaper abrasion with the use of sandpaper grit sizes 220, 320, 500, 800, 1000, 2400, polishing with the use of diamond paste of 3 and 1 $\mu$ m particle size. After preparing the samples, coatings were analysed through measuring characteristic spots of the outline as indicated in Fig. 1. Photographs of the microstructure were taken, the coating thickness and chemical composition in selected spots were measured. For purposes of the research the following equipment was used: a NIKON Epiphot 300 optical microscope, a HITACHI S-3400N scanning electron microscope with EDS Thermo system for microanalysis of chemical composition.

## 3. Results

### 3.1. Results of thickness measurements and the aluminide coating's chemical composition analysis

The research has proven that the entire surface of a blade was aluminide-coated. Discontinuities in the coating have been reported. The coating's microstructure in selected spots have been presented in Fig. 2. Thickness measurements have shown significant differences in the coating's thickness of the blade profile. It has been reported that the thickest coating has been formed on the leading and trailing edge of the blade - above 40  $\mu$ m. In other spots - that is the platform and blade top area - the aluminide coating was thinner and ranged from 31 to 37  $\mu$ m (Fig 3, Table 2, Fig 4). The thinnest coating was reported in the bottom part of the trailing edge - 31  $\mu$ m. A chemical composition analysis performed on the coating's section close to the leading edge has shown a decrease in aluminium content (Fig. 4, Table 2).

Table 2.  
Results of the chemical composition analysis in areas shown in Fig. 4, % at.

Area	Al	Ti	Cr	Co	Ni	Mo	W
1	50.92	0.13	0.75	1.91	46.29	-	-
2	49.84	-	0.89	2.50	46.53	-	0.24
3	43.96	1.95	5.04	3.54	43.98	0.69	0.84
4	50.47	-	1.01	2.59	45.55	-	0.37
5	11.02	3.37	11.25	4.51	65.28	2.33	2.24
6	31.78	5.02	8.64	3.94	48.61	1.23	0.78

The aluminium amount decreased on average from 50.92% to 43.96% at. The nickel content is also lower: area 1 - 46.29% at., area 2 - 46.53% at., area 3 - 43.98% at., while the cobalt amount rises accordingly to 1.91%, 2.5%, 3.54%. The titanium content rises gradually towards the alloy base. In the contact area some typical releases were reported (point 6 in Fig. 4). An analysis of their chemical composition revealed increased chromium content (8.64%). The chemical composition analysis carried out beyond the coating proved the base material to be in accordance with its chemical composition (Table 3).

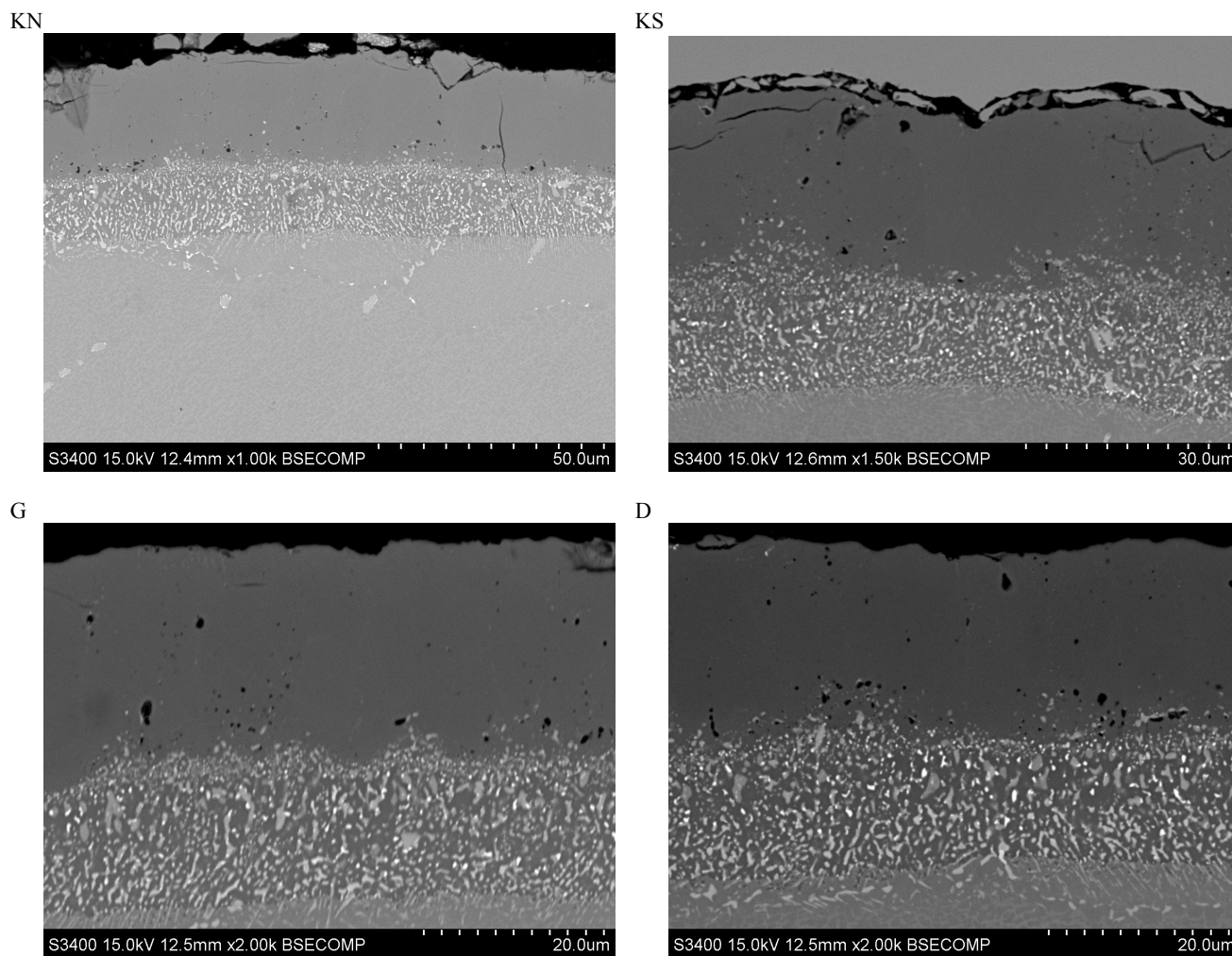


Fig. 2. The aluminide coating’s microstructure as observed in the leading edge area (KN), the trailing edge (KS), the top (G) and the platform (D)

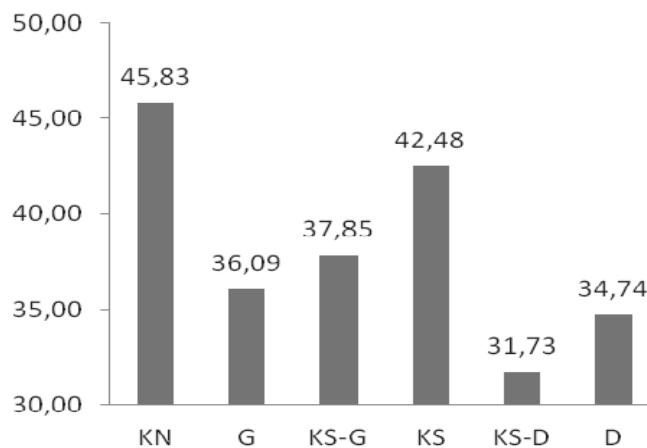


Fig. 3. Aluminide coatings’ thickness in selected spots as indicated in Fig. 1

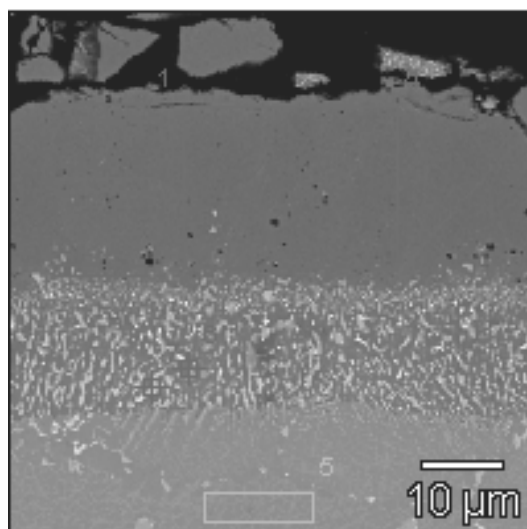


Fig. 4. Selected spots for chemical composition analysis in the leading edge area of a ZS6K-alloy blade after aluminisation

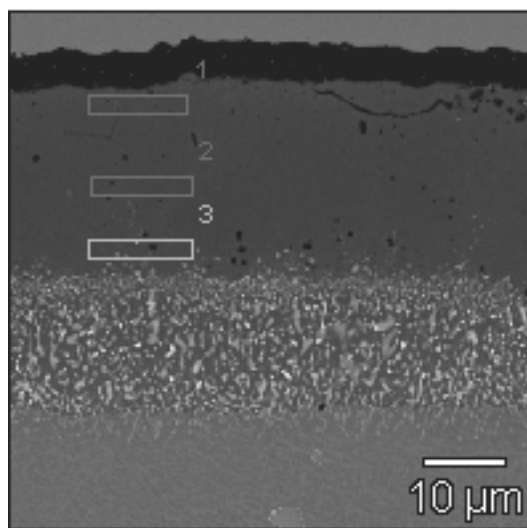


Fig. 5. Spots selected for chemical composition analysis in the platform area of the ZS6K alloy blade after aluminisation

Table 3. Results of the chemical composition analysis in the areas indicated in Fig. 5, % at.

Area	Al	Ti	Cr	Co	Ni
1	52.04	-	0.61	1.71	45.63
2	50.19	-	0.83	3.08	45.90
3	50.05	-	0.97	3.17	45.00

Similarly to other investigated spots, aluminium content measured in measurement spot in the blade top area (G) falls

towards the alloy base and stands at approx. 50% (Fig. 5). Nickel content changes only slightly across the coating section (approx. 45%). An increase in the chromium and cobalt content towards the alloy base can also be observed. In area 3 some amount of titanium can be observed - 0.79%.

Measurements of the aluminium content in all points of the outer layer (Table 4) have shown that the layer is homogenous and equals from 50 to 52 at. %, what attests to homogeneity of the chemical composition of aluminide coating in the blade section.

Table 4. Results of chemical composition analysis in the external layer of all spots indicated in Fig. 1

	Aluminium amount, at %					
	KN	G	KS-G	KS	KS-D	D
VPA	50.92	52.04	50.92	51.42	51.24	50.79

### 3.2. Results of thickness measurements and chemical composition analysis of the ceramic coating

Performed processes of ceramic coating deposition with the use of PS-PVD method showed coating of the entire blade except for the lock area. The ceramic coating microstructure of the blade section can be seen in Fig. 7. Significant changes were observed - column crystals were thinner and higher. In the internal part of the blade (a platform close to the trailing edge), coating is thinner. In the trailing edge area faults of the ceramic coating structure were found. These will not ensure protection of the blade surface.

Measurements have shown significant differences in the ceramic coating thickness (Fig. 6).

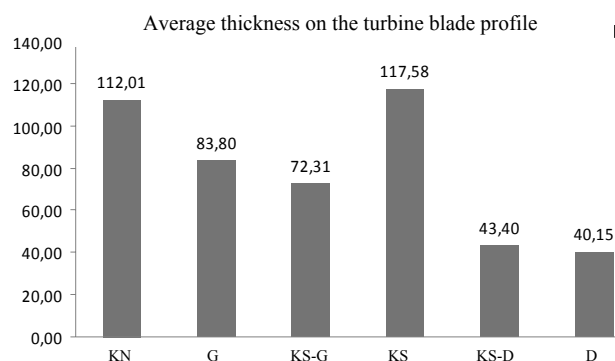


Fig. 6. Measurement results for ceramic coating thickness of the thermal barrier as in spots indicated in Fig. 1

The thickest coating was observed in the leading and trailing edge of the blade (>100 μm). Within the blade top area (G and KS-G points) the coating thickness equaled 73-84 μm. The thinnest part of the blade was observed within the platform area - circa 40 μm.

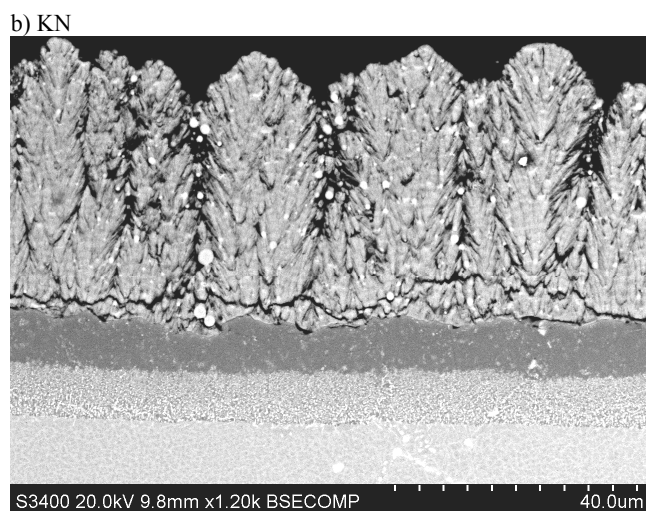
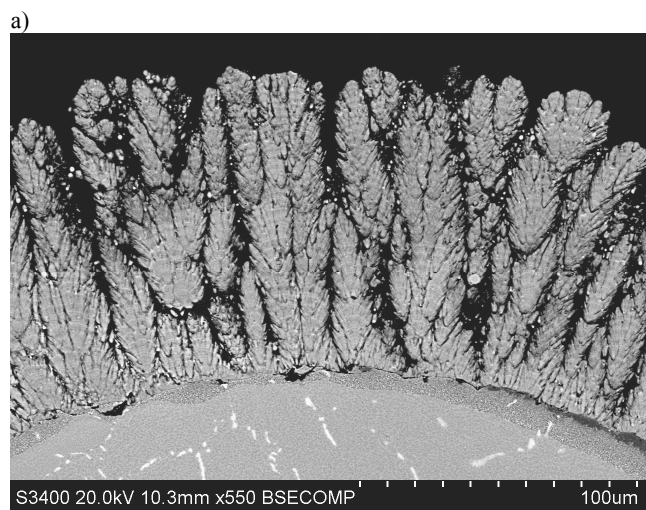


Fig. 7. Morphology of the ceramic coating of the turbine blade made of ZS6K alloy, aluminide-coated on the leading edge (a) and the platform (b)

#### 4. Summary

Technological tests have shown an ability to form thermal barrier coating on modelled turbine blades. In this research typical diffusion aluminide coating was formed as an interlayer in the gas phase aluminising method. Measurements of aluminium content have revealed homogeneity of the coating's chemical composition and significant differences in its thickness. The thickest coating was observed in leading and trailing edge of the blade (above 40  $\mu\text{m}$ ), whereas in other parts of the blade it was thinner (between 30 and 40  $\mu\text{m}$ ). Observed differences agree with results given in literature on the subject [3]. Differences in thickness were also observed in the deposited ceramic coating. The thickest coating exceeding 100  $\mu\text{m}$  was observed in the trailing edge of the blade, while the thinnest coating was found in the platform.

Differences in thickness result from the PS-PVD process as well as equipment used for the procedure. During this process, a component moves in the plasma flow and this causes a strong impact of the element geometry and the used equipment on the coating structure. The equipment allowed for rotation of two blades placed opposite one another, which caused the observed 'shade' close to the blade lock. In the future it may occur that entirely different equipment as well as software for steering of the manipulator and plasma burner will be necessary in order to reduce differences in the coating thickness.

#### Acknowledgements

Financial support of Structural Funds in the Operational Programme - Innovative Economy (IE OP) financed from the European Regional Development Fund - Project "Modern material technologies in aerospace industry", Nr POIG.01.01.02-00-015/08-00 is gratefully acknowledged.

#### References

- [1] A. Onyszko, K. Kubiak, J. Sieniawski, Turbine blades of the single crystal nickel based CMSX-6 superalloy, *Journal of Achievements in Materials and Manufacturing Engineering* 32/1 (2009) 66-69.
- [2] M. Hetmańczyk, L. Swadźba, B. Mendala, Advanced materials and protective coatings in aero-engines application, *Journal of Achievements in Materials and Manufacturing Engineering* 24/1 (2007) 372-381.
- [3] A. Squillace, R. Bonetti, N.J. Archer, J.A. Yeatman, The control of composition and structure of aluminide layers formed by vapour aluminizing, *Surface and Coating Technology* 120-121 (1999) 118-123.
- [4] A.B. Smith, A. Kepster, J. Smith, Vapour aluminide coating of internal cooling channels in turbine blades and vanes, *Surface and Coating Technology* 120-121 (1999) 112-117.
- [5] Wen-Pin Sun, H.J. Lin, Min-Hsiung Hon, CVD aluminide nickel, *Metallurgical Transaction* 17/2 (1986) 215-220.
- [6] I. Gurrappa, Identification of hot corrosion resistant MCrAlY based bond coatings for gas turbine engine application, *Surface and Coating Technology* 139/2-3 (2001) 272-283.
- [7] W.A. Nelson, R.M. Orenstein TBC experience in land-based gas *Journal of Thermal Spray Technology* 6/2 (1997) 176-180.
- [8] J. Singh, D.E. Wolfe, J. Singh, Architecture of thermal barrier coatings produced by electron beam-physical vapor deposition (EB-PVD) *Journal of Materials Science* 37/15 (2002) 3261-3267.
- [9] M.O. Jarligo, D.E. Mack, R. Vassen, D. Stöver, Application of plasma-sprayed complex Perovskites as thermal barrier coatings, *Journal of Thermal Spray Technology* 18/2 (2009) 187-193.
- [10] Y. Yang, H. Liao, Ch. Coddet, Simulation and application of a HVOF process for MCrAlY thermal spraying, *Journal of Thermal Spray Technology* 11/1 (2002) 36-43.

- [11] B. Rajasekaran, G. Mauer, R. Vaßen, Enhanced characteristics of HVOF-sprayed MCrAlY bond coats for TBC, *Applications Journal of Thermal Spray Technology*, 20/6 (2011) 1209-1216.
- [12] G. Moskal, Thermal barrier coatings: characteristics of microstructure and properties, generation and directions of development of bond, *Journal of Achievements in Materials and Manufacturing Engineering* 37/2 (2009) 323-331.
- [13] O. Altun, Y. Erhan Boke, A. Kalemtaş, Problems for determining the thermal conductivity of TBCs by laser-flash method, *Journal of Achievements in Materials and Manufacturing Engineering* 30/ 2 (2008) 115-120.